HiSST: 2nd International Conference on High-Speed Vehicle Science & Technology
11–15 September 2022, Bruges, Belgium

Design and testing of a low mass flow RDE running on ethylene-oxygen

Hamilton Law[1], Tom Baxter[1], Charlie Ryan[1,2], Ralf Deiterding[1,3]

Abstract

A modular laboratory rotating detonation engine (RDE) for combined mass flow rates below $10\,\mathrm{g/s}$ has been designed. Since a large chamber diameter to width ratio is used, first tests with stoichiometric ethylene-oxygen mixtures have revealed detonation modes with one, two and three separate detonation heads, depending on mass flow rate. Spectrograms from high-frequency pressure data and high-speed photography are used to confirm successful operation and identify the operational modes reliably.

Keywords: *rotating detonation engine experiment, ethylene-oxygen, minimal chamber design*

Nomenclature

Latin

A_c – Combustion chamber area
d_c – Diameter of outer chamber
d_i – Diameter of insert
F – Thrust of the RDE
h – Combustion chamber width
I_{sp} – specific impulse of the RDE
K – Ratio of det. length to mixture layer depth
L_c – Combustion chamber length
L_{cr} – Critical mixture layer depth
l – Length between successive detonation fronts
$\dot{m}$ – Total mass flow rate
p – Pressure of the unreacted gas mixture
R – Specific gas constant of the unreacted mixture
T – Temperature of the unreacted gas mixture
t_d – Cycle time between detonation fronts
U_d – Detonation velocity
V – Volume of combustion chamber
v_{inj} – Outflow velocity from fuel injectors
w – Detonation number in combustion chamber

Greek

λ – Lateral detonation cell size
λ_{ref} – Cell size at a reference pressure p_{ref}

1. Introduction

A rotating detonation engine utilises a detonation wave which travels azimuthally within an annular chamber to expel propellant and generate thrust. The chamber is determined by two coaxial cylinders, and the radial gap between them, referred to here as the chamber width, forms the chamber. Detonation waves are maintained by constantly feeding fuel and oxidiser into the chamber, thus ensuring that there is a constant mixture of reactants in front of each detonation wave.

RDEs are of interest due to their potential efficiency gains in hypersonic propulsive systems. The efficiency gains of a detonation engine are due to the greater temperature and pressure increase produced by detonation over deflagration, allowing more work to be extracted from the same amount of propellant. While the first stationary spinning detonation was successfully achieved in 1963 [1], continuous detonation propulsion has seen increased interest only in recent years. The study of RDEs is currently underway in Russia, Poland, France, China, USA, Japan, Germany [2, 3]. To the best of our knowledge, this paper reports on the first successful RDE experiments in the UK. Constructed as a small-scale laboratory demonstration project, the objective was to utilize as small mass flow rates as possible. This naturally lead to the adoption of a RDE rocket design supplied with pure oxygen. For safety and ease of handling ethylene was selected as fuel.

[1] *Department of Aeronautics & Astronautics, University of Southampton, Boldrewood Innovation Campus, Southampton, SO16 7QF, United Kingdom*
[2] *c.n.ryan@soton.ac.uk*
[3] *r.deiterding@soton.ac.uk*

The University of Southampton's RDE differs from previous designs in a variety of ways. Firstly, it is small, with a combustion chamber outer diameter of only $75\,\mathrm{mm}$, roughly half the $150\,\mathrm{mm}$ of a typical laboratory RDE [4]. The small size poses some benefits, safety and portability for example, but also some challenges. The theoretical Chapman-Jouget (CJ) velocity of stoichiometric ethylene and oxygen is approximately $2500\,\mathrm{m/s}$, therefore with a smaller diameter chamber the detonation has a shorter distance to travel before reaching the same location once more, imposing challenging refresh rates and mixing times. This leads to a requirement of rapid filling for sustaining a continuous detonation. The use of ethylene as a fuel is also comparably unusual. The majority of RDEs studied thus far use hydrogen or methane [2], predominantly due to their prevalence in rocketry. Furthermore, the mass flow rate of the propellants supplied during successful operation, as demonstrated in Section 3.2 is significantly lower than that of larger RDEs.

Additionally, this RDE is particularly modular, as will be described further in Section 2.1. The injector plate can be varied, as can the chamber width and a number of other geometric parameters. Furthermore, a variety of aerospike nozzles can be attached, with a choice of nozzle half-angles, axial throat position, and throat area. The chamber width can be varied depending on the insert selected; during the experiments described it was $0.7\,\mathrm{mm} - 1.2\,\mathrm{mm}$. This small chamber width relative to the $75\,\mathrm{mm}$ diameter minimises the influence of curvature and is expected to aid in stabilising the detonation. Furthermore, the large ratio of circumferential chamber length compared to the width allows for multiple simultaneously sustained detonation heads, as can be seen in the experimental data.

Finally, this project is the culmination of three years work carried out by three teams of Masters students at the University of Southampton. The first cohort developed the initial design and sizing of the RDE, and submitted these parts for manufacture. The second group developed the pre-detonator and propellant delivery system. In the final year, both the aerospike and thrust stand were designed and manufactured, and the propellant delivery system and laboratory set up improved, before testing could begin.

In Section 2 we report on the fundamental design considerations for the sizing of our RDE. Section 3 gives first results, where we demonstrate successful operation at total mass flow rates as low as $3.5\,\mathrm{g/s}$. The conclusions are given in Section 4.

2. Design

2.1. Chamber design and sizing

2.1.1. Design equations

The sizing of rotating detonation engine chambers is based primarily on the lateral size of a detonation cell λ that a Chapman-Jouguet detonation, travelling through the mixture in free space, would exhibit. Experimentally, it has been established that the detonation cell size is approximately inversely proportional to the pressure of the unreacted mixture, p, giving

$$\lambda = \frac{\lambda_{\mathrm{ref}} p_{\mathrm{ref}}}{p}, \tag{1}$$

where p_{ref} and λ_{ref} are a chosen reference pressure and its corresponding, experimentally measured, cell size for a given propellant combination. A large number of detonation cell size measurements has been compiled for instance in the Caltech detonation cell database [5].

Particularly useful for minimal chamber design are the relations by Kiyanda et al. [6]. First, the chamber width h must allow for a minimum number of detonation cells to exist within the annular channel:

$$h \geq (2.4 \pm 1)\lambda \tag{2}$$

In addition, there exists a minimum mixture layer depth, known as the *critical* mixture depth, which will sustain detonation propagation:

$$L_{cr} = (12 \pm 5)\lambda \tag{3}$$

As highlighted by Eq. (1), a higher chamber pressure reduces the detonation cell size, thus allowing more cells to fit within the geometry and increasing the likelihood of successful detonation. For selecting a

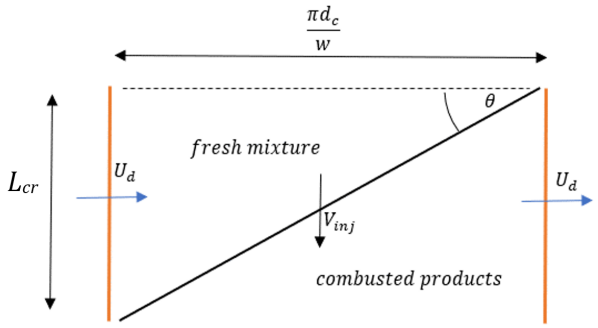

Fig 1. Detonation wave propagation in an unrolled annulus chamber.

suitable chamber length Bykovskii et al. [7] found that there exists a minimum chamber length $L_{c_{\text{min}}}$ of $2L_{cr}$. However, they also found that a chamber length smaller than $3L_{cr}$ leads to inefficient operation due to incomplete combustion and thus, an optimal chamber length of $L_{c_{\text{opt}}} \geq 4L_{cr}$ was identified. To select a suitable diameter for the RDE, a geometric parameter K in addition must be satisfied. K is defined as

$$K = \frac{l}{L_{cr}} = \frac{\pi d_c}{w L_{cr}}, \tag{4}$$

where l is the length between successive detonation fronts, d_c is the diameter of the outer wall of the chamber and w is the wave number or number of detonation waves within the chamber. Bykovskii et al. showed through experimentation that K is roughly constant for all annular cylindrical combustion chambers where a gaseous oxidiser is being used, and found $K = 7 \pm 2$ [7]. In order to sustain at least one detonation wave reliably a minimum diameter of

$$d_{c_{\text{min}}} = \frac{L_{cr} K}{\pi} \tag{5}$$

needs to be used. Therefore with the equations above, the width, length and diameter of the RDE combustion chamber can be defined.

Finally, for any selected design one must confirm that a stable detonation can be housed; i.e., that the wave number w is at least 1. To derive an expression for the wave number, the annular chamber of the RDE is "unrolled" into a strip, cf. Fig. 1. Here, the detonation waves move from left to right at a speed U_d, the distance $l = \frac{\pi d_c}{w}$ is between two successive detonation fronts. In the case that only a single detonation ($w = 1$) is present in the combustion chamber, the bottom detonation is seeing the back of its own reaction zone. The combustible mixture is injected from the top and has a velocity v_{inj}. The amount of reactant grows from zero, at the point of the previous detonation to L_{cr} at the point of the following detonation. The angle θ can therefore be expressed in two ways:

$$\tan(\theta) = \frac{v_{\text{inj}}}{U_d} = \frac{L_{cr}}{\frac{\pi d_c}{w}} \tag{6}$$

We can evaluate the injection velocity as $v_{\text{inj}} = \frac{\dot{m}}{\rho A_c}$, where the area of the chamber is $A_c = \pi d_c h$ with h, the chamber width. ρ is the density and $\dot{m}$ the mass flow of the combustible mixture. Finally, v_{inj} can be substituted into Eq. (6) and the two relations equated to give an expression for the wave number:

$$w = \frac{\dot{m}}{\rho L_{cr} U_d h} \geq 1 \tag{7}$$

Substituting Eq. (3), Eq. (1) and the ideal gas law, we reach the final form

$$w = \frac{\dot{m} R T}{(12 \pm 5) \lambda_{\text{ref}} P_{\text{ref}} U_d h} \geq 1, \tag{8}$$

where R and T are the specific gas constant and the initial temperature of the unreacted combustible mixture, respectively.

Table 1. Selected design conditions for an RDE running on stoichiometric ethylene-oxygen at $\dot{m} = 5\,\mathrm{g/s}$.

p [bar]	λ [mm]	h [mm]	L_{cr} [mm]	$d_{c_{\mathrm{min}}}$ [mm]	w
1	0.465	0.651-1.581	3.255-7.905	5.18-22.65	0.18-0.75
2	0.233	0.323-0.791	1.628-3.953	2.59-11.33	0.36-1.51
3	0.155	0.217-0.527	1.085-2.635	1.73-7.55	0.54-2.255

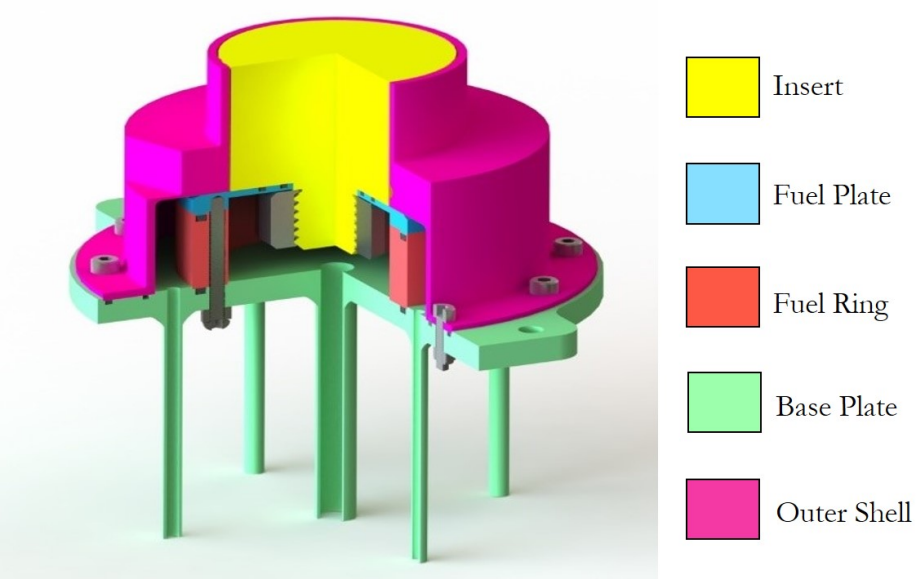

Fig 2. The University of Southampton RDE design

2.1.2. Propellant Selection

The key requirement with regards to propellant selection was for a small cell size, to enable the design of a suitably small RDE. Throughout the selection process the small mass flow rate of the available propellant delivery system and using only bottle pressure to drive the propellants posed significant limitations. It was estimated from previous experience and expected volumetric flow rates that the delivery system was capable of a combined mass flow rate of $5 - 10\,\mathrm{g/s}$. A number of fuels and oxidisers were proposed including methane, hydrogen, acetylene or ethylene as fuels, and air or oxygen as an oxidiser. Initially, a gaseous acetylene-oxygen selection was pursued, as it produced the smallest estimated cell size, of $0.18\,\mathrm{mm}$ at $1\,\mathrm{bar}$ mixture pressure, however acetylene was found to require a manifold cylinder array. Hydrogen had to be ruled out for safety reasons. Hence, ethylene-oxygen became an eventual natural choice, with an estimated cell size of $0.465\,\mathrm{mm}$ at $1\,\mathrm{bar}$ [5]. Table 1 summarizes the range of minimum and maximum design conditions for an RDE running on stoichiometric ethylene and oxygen at $\dot{m} = 5\,\mathrm{g/s}$ and $T = 298\,\mathrm{K}$ and for an estimated detonation speed of $U_d = 2500\,\mathrm{m/s}$. In Table 1, w gives the number of expected detonation waves within the chamber.

A fixed chamber diameter of $d = 75\,\mathrm{mm}$, clearly larger than $d_{c_{\mathrm{min}}}$ of any of the cases in Table 1, was selected to minimize curvature effects and increase the likelihood of successful operation. The chamber diameter d is defined by the Outer Shell. A modular design with different inserts allows for inner chamber heights L between 35 and $50\,\mathrm{mm}$ and chamber width h of $0.7\,\mathrm{mm}$ to $1.2\,\mathrm{mm}$. It is imminent from Table 1 that ensuring a sufficient pressure p of the unreacted gases can be of vital importance for successful operation. Therefore, constrictor end plates with slightly increased diameter, acting as a nozzle at the chamber outlet, were incorporated into the design and can be attached to the insert. In addition, a variety of aerospikes, with a choice of nozzle half-angles and axial throat positions have been designed to enhance thrust, cf. Section 2.3.

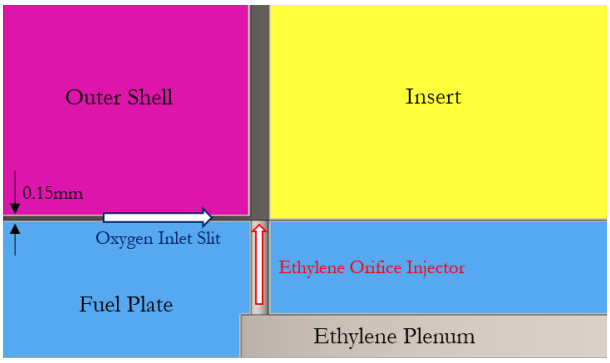

Fig 3. Close up showing injector design, with tangential oxygen flow through the circumferential slit and ethylene through axial orifice injectors

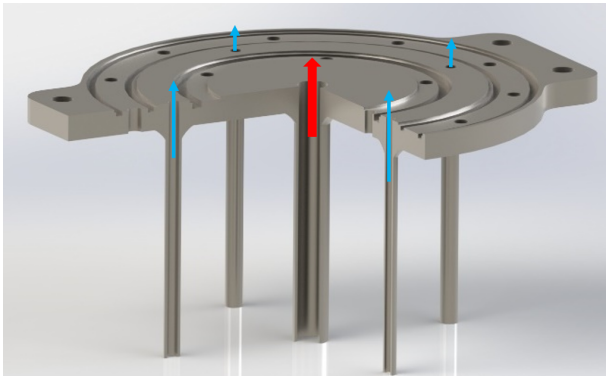

Fig 4. Baseplate design with ethylene shown in red, and oxygen shown in blue

It is clear from the Table 1 that the wave number, and therefore success of the engine, can vary significantly, depending on chamber width (driven by cell size and thus pressure), the true critical layer depth, detonation velocity, and mass flow rate provided. Many of these variables are difficult to predict in advance and therefore the modularity of the design was intentional to allow for tuning of the RDE specification throughout the test campaign. Furthermore, it would enable any future researchers to readily experiment with different configurations of the design. The design selected is shown in Figure 2. 313 Stainless steel was chosen for the manufacture of this RDE, due to its relatively high melting and relation temperature, and ease of procurement.

2.1.3. Injector Design

Having selected a suitable chamber design, the next key aspect to consider was injector design. For safety reasons, ethylene and oxygen mix only in the detonation chamber. A number of options were considered such as jets in crossflow, semi-impinging jets and pintle injectors [8]. Ultimately, a variant of jets in crossflow was selected, where ethylene would be inserted axially using simple orifice injectors in an exchangeable fuel plate, and the oxygen would be introduced in a cross flow, around the full circumference of the RDE, through a small slit produced between the Fuel Plate and Outer Shell, Fig. 3. This method was selected due to its proven success in a modular RDE by Shank [9]. The ethylene plenum is filled by one central pipe and the oxygen plenum via four pipes distributed evenly around the baseplate circumference to encourage an even oxygen distribution, cf. Fig. 4. The two plenum volumes are separated by the Fuel Ring and Fuel Plate, with the interface between these components sealed by a series of o-rings.

The key requirement for the injector design is that suitable filling, to at least the critical depth, and mixing in a certain region of the chamber, must occur before the detonation reaches that region - to sustain

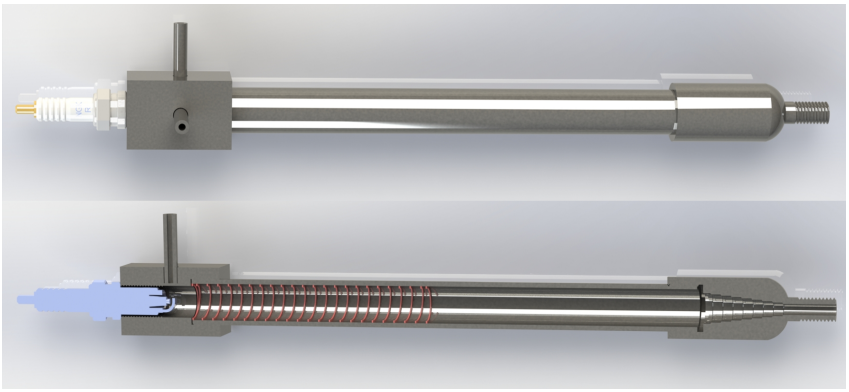

Fig 5. Predetonator design, with section view including Schelkin Spiral highlighted in red

the continuous operation. Suitable mixing should be achieved by the jets in crossflow configuration, however filling relies on volumetric flow rate and propellant velocity. The required fill velocity was found through first calculating the required fill volume, where d_i is the diameter of a given insert:

$$V = \frac{\pi(d_c^2 - d_i^2)L_{cr}}{4} \tag{9}$$

Next, the cycle time t_d between detonation fronts can be estimated from the detonation velocity U_d and the perimeter of the chamber. Although the theoretical CJ velocity for a detonation is an overestimate, with experimental RDE results showing the detonation speed is usually between 60-85% of the CJ speed, this provides a useful scenario to find the maximum volumetric flow rate required [10]:

$$t_d = \frac{\pi d_c / w}{U_d} \tag{10}$$

Thus, from Eqs. (9) and (10) the required volumetric flow rate, $\dot{V}$, can be readily estimated. In line with the modular approach, injector plates with 30, 45 or 60 orifice injectors were manufactured, all with 0.5 mm orifice diameters. Note that an orifice diameter in the order of the expected detonation cell size reduces the chance of flashback through the system reliably. For each injector-oxygen slit-chamber configuration, with a given equivalence ratio, the volumetric flow rate for oxygen and ethylene can be found, then the required velocity/mass flow rate can be computed from the respective injector area.

2.2. Predetonator

To initiate the engine a predetonator (PD) is used, which is once again modular. This is fundamentally a tube with a spark plug at the closed end and an open end injecting into the chamber. The PD is initially filled with reactants, which are then ignited by the spark, producing a deflagration. As the deflagration travels along the tube it will accelerate and undergo deflagration-to-detonation transition (DDT), provided the tube is of sufficient length. The detonation can then be tangentially injected into the pre-filled main chamber, to begin the continuous rotating detonation operation. This PD is not essential, and RDE have been ignited directly in the main chamber channel with a spark, forming a deflagration that eventually becomes a detonation over an effectively infinite distance[4]. However, since the spark plug ignites in a relatively open area, flame fronts will propagate both clockwise and counter clockwise around the chamber, making detonation establishment less reliable.

For sizing of the PD, once again, detonation cell size is of great importance. Mitrofanov et al. found that the tube diameter must be at least 13λ in order for the detonation to propagate [11]. For a stoichiometric ethylene-oxygen mixture at 1 bar, this results in a minimum PD diameter of 6.045 mm. Given that pipes are readily available in standard sizes of both 10 mm and 16 mm these sizes were selected for testing. Additionally, James [12] found that the minimum tube length for DDT to occur with ethylene-oxygen

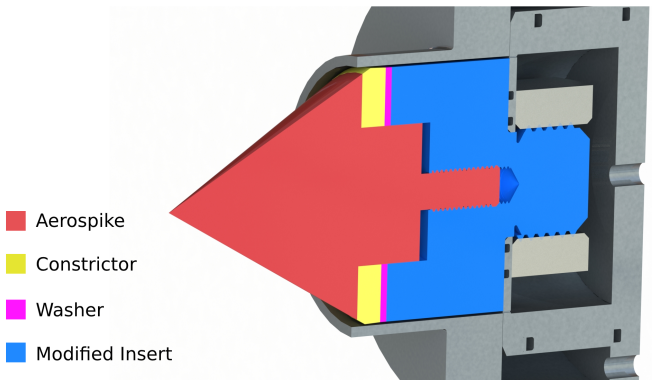

Fig 6. Modular aerospike nozzle design

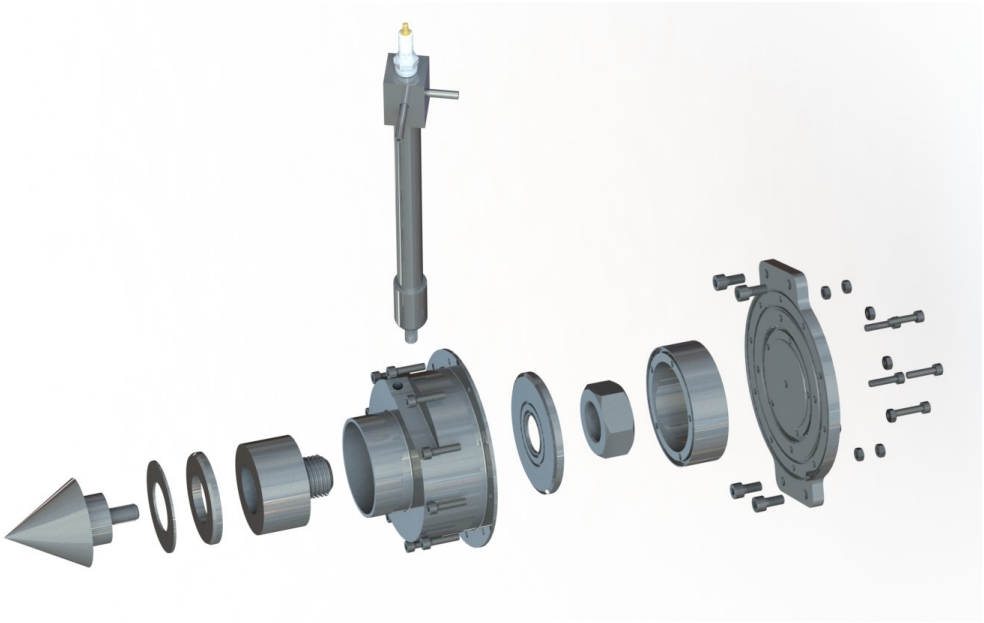

Fig 7. Exploded view of the entire University of Southampton RDE design

is three times the tube diameter, thus 30 mm or 48 mm for our design. As this is a fairly empirical minimum, predetonator tubes of 120 to 320 mm length were produced.

DDT is not only dependant on the selected propellants, their equivalence ratio and pipe dimensions. Hasson et al. [13] also demonstrated that the energy imparted by the spark has a significant impact and Shchelkin reported that spirals obstructing a deflagration's passage through a pipe could accelerate the DDT, with these DDT enhancement tools becoming known as Shchelkin spirals [14]. This is caused by the spiral increasing perturbations to the deflagration flame front, producing kernels of high temperature and pressure of local ignition that accelerate the deflagration. For sizing of a Shelkin spiral the most important parameter is the blockage ratio, which is the ratio between the cross sectional area of the spiral blocking the tube and the internal cross-sectional area of the tube. After evaluating a number of these spirals by empirical two-dimensional numerical simulation, a spiral of length 103.87 mm, pitch 4.74 mm and coil thickness 3.18 mm was manufactured, equating to a blockage ratio 39% when used with the nominal 16 mm diameter PD, cf. Fig. 5.

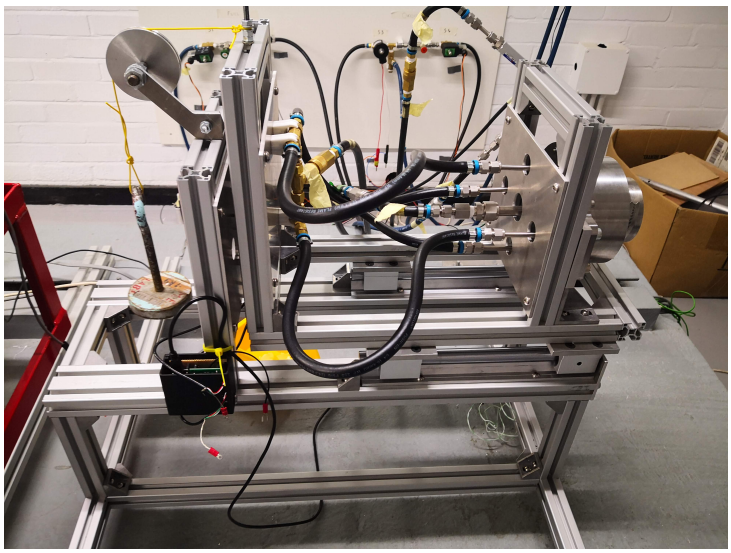

Fig 8. Thrust stand during calibration

2.3. Nozzle attachments

As mentioned previously, in order to ensure a sufficient internal pressure p, constrictor end plates with slightly increased diameter, acting as a nozzle throat at the chamber outlet, can be attached to the insert, cf. Fig. 6. Three constrictors were manufactured producing throat areas of $122.8\,\text{mm}^2$, $82.11\,\text{mm}^2$ and $41.1\,\text{mm}^2$ respectively. Naturally the throat-to-chamber area ratio varies depending on the selected Insert and thus chamber width. Additionally, the axial position of the throat can be varied, to be recessed into, or extended out of, the Outer Shell, through the stacking of $2\,\text{mm}$ thick washers between the Insert and Constrictor.

Furthermore, a variety of toroidal aerospike nozzles have been manufactured. The aerospike design integrates naturally into the annular RDE topology and their performance has also been demonstrated in this context, cf. [15, 16]. As shown in Fig. 6, the aerospikes are conical in shape. Half angles of 35°, 30° and 25° have been manufactured, producing nozzles with a range of lengths. These values were chosen based upon preliminary CFD studies indicating that a 30° conical aerospike would most greatly increase thrust, the other two nozzles were proposed to provide comparative cases. An exploded view of entire engine design, including aerospike nozzle and predetonator, is shown in Fig. 7.

2.4. Thrust stand

To determine the thrust generated, a stand that allows motion along linear rails was also designed. It is equipped with two cantilever loads cells capable of measuring a total maximal force of $58.84\,\text{N}$, i.e. $24.42\,\text{N}$ for each load cell. The thrust stand was manufactured from aluminium extrusion due to is ubiquity and stiffness. The final assembled thrust stand, along with linear rails, and RDE mounted can be seen in Fig. 8.

Using a mass and pulley system, with the cable attached to the rolling section of the thrust stand, as shown on the left of Fig. 8, the accuracy of the thrust measurements was determined. Masses were applied and the force read by the load cells recorded. The results of this testing can be seen in Fig. 9. The figure shows that generally there is good agreement between the applied mass and the recorded mass, particularly with the lowest masses applied. With greater applied mass, the mass recorded by the load cells has been shown to increasingly under-read, from good agreement at $50\,\text{g}$ to a -7.9% under-valuation when $220\,\text{g}$ was applied. This trend continued as successively larger masses were applied, rising to a -15.2% under-valuation with $1.9\,\text{kg}$ applied. However, the maximum experimental thrust recorded was $\sim 1\,\text{N}$ or $\sim 102\,\text{g}$, thus only the region of interest is shown. Further results of the experimental thrust data can be found in Section 3.3.

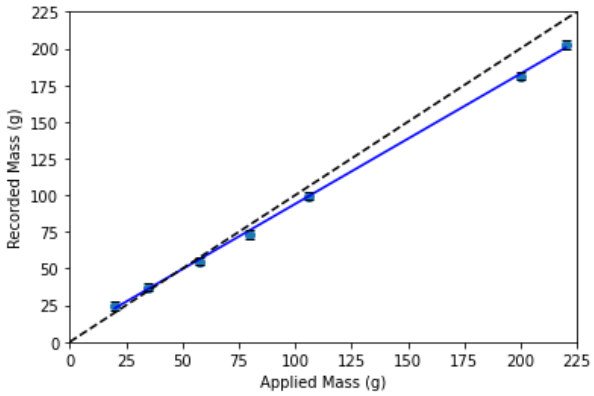

Fig 9. Agreement between applied mass and mass read by thrust stand. Error bars represent one standard deviation. Dashed line highlights linear relationship.

2.5. Laboratory setup

The laboratory setup consists of a control PC running LabVIEW software, with a National Instruments DAQ system providing the interface between the PC, fluid control system and instrumentation. The fluid control system is relatively simple in design. It was built by adapting an existing system designed for a gaseous bi-propellant rocket engine. It features basic mass flow control by needle valves, digital mass flow meters and control solenoids. The RDE combustion chamber and predetonator have their own supply lines, as can be see in Fig. 8, allowing mass flow rate to be varied independently between them for best reliability and performance.

The LabVIEW control software is key to the RDE's operation, allowing precise and repeatable control of the various solenoid valves and spark plug, as well as a centralised data acquisition system. This gathers and stores data from mass flow meters, high frequency pressure transducer, thermocouple and load cells. The software is designed to completely automate the RDE's operation. Once the valve timings are set, the operator have no further input other than starting the code. The entire startup, running and shutdown procedure, including nitrogen purging, is entirely automated. This allows repeatable RDE operation to within 1 ms.

The control panel of the LabVIEW software is shown for illustration in Fig. 10. This shows a live data readout from all sensors, solenoid valve positions, valve and spark plug timing settings and measured valve timings during operation.

3. Test results

3.1. Instrumentation

To successfully identify and characterise RDE behaviour suitable instrumentation is required, to capture the high-frequency and somewhat unstable nature of detonation propagation. For this RDE, the key instruments used to show this behaviour were a high-frequency pressure transducer and a Phantom high-speed camera.

The pressure transducer selected was a PCB dynamic pressure sensor, which utilises a piezoelectric crystal to show transient pressure behaviour. Since the expected detonation height is in the range of just a few millimetres, cf. L_{cr} in Table 1, it is intrinsically difficult to place the transducer entirely into the detonation zone and accurately measure the Chapman-Jouguet, not to mention the von Neumann pressure, of the actual detonation wave. Instead, in our small-scale design, the transducer–despite being mounted as close to the chamber bottom as possible–is used effectively as a high-frequency contact microphone. The pressure transducer output was high-pass filtered at a frequency of 100 Hz to remove interference from AC power, and then Fourier transformed in small discrete sections to produce a spectrogram.

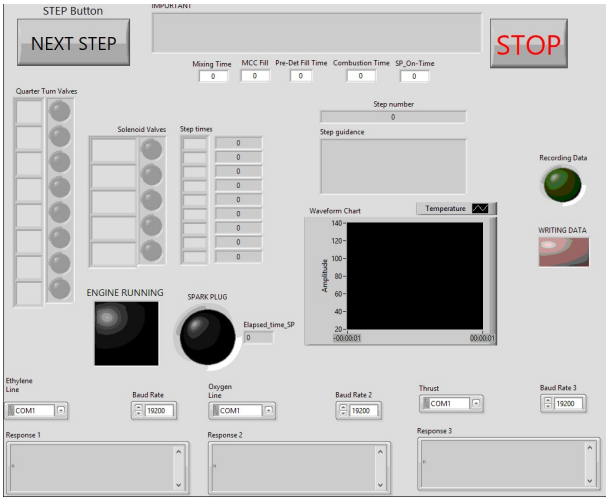

Fig 10. User interface for the RDE control software built in LabVIEW

During the testing process, various methods were explored to ascertain whether detonation was occurring, and differentiate between detonation behaviour, and any particular resonances or flame instability in the flow. A solution was found by the use of a high-speed camera, using a 53 kHz frame rate. Whilst a higher frame rate would have been preferable to show the detonation locations more precisely, a relatively long shutter speed of $17\,\mu$s was required for the detonation fronts to show up clearly in the footage and a faster frame rate would have required a faster shutter speed. As a result, the fronts are not clearly defined, but instead appear as a long tail, the length of which corresponds to the distance travelled by the detonation front in the $17\,\mu$s shutter time. While this is not a perfect solution, it still allows a clear distinction between detonative and deflagrative behaviour, including visualising transient detonation behaviour in reasonable detail, such as ignition behaviour, the transition to a stable detonation regime. Most importantly, the high-speed images allow unambiguous identification of the number detonation fronts at a specific time instant.

3.2. Variation of mass flow rate

First successful tests used a chamber width of $h = 1.2$ mm, stoichiometric fuel-oxygen conditions and no additional nozzle. The flame patterns during test runs with total mass flow rates of 9.7 g/s, 6.6 g/s, and 3.5 g/s are shown in Fig. 11. The chamber outlet of the engine, its mounting on the thrust stand, as well as the predetonator can be seen on the right. The difference in flame pattern for these considerably different mass flows rates is apparent, with the intensity decreasing with mass flow rate and colouration of the flames changing from orange to blue. Snapshots from the high-speed footage reveal that in the 9.7 g/s case, Fig. 12a, three separate detonation wave heads co-rotate in the engine, while in the 3.5 g/s case, Fig. 12c, only a single detonation wave can be identified. For the 6.6 g/s case, Fig. 12a, two co-rotating heads can be seen, however at this mass flow rate the footage indicated that the number of detonation heads would frequently switch between two and three. This is supported by the corresponding spectrogram in Fig. 13b, where there are two dominant frequencies at approximately ~ 17.5 kHz and ~ 15 kHz.

The spectrograms of Fig. 13 further reveal a startup phase until approximately ~ 1.7 s for all cases and reliable detonation operation thereafter. We believe the startup perturbances to originate from firing a predetonator into a combustion chamber that has roughly only $1/5$ of the predetonator volume. In the second half of the experiment reliable unperturbed detonation circulation is established. In the upper spectrogram of Fig. 13a a dominant frequency of ~ 19.22 kHz is found, which for three rotating detonation fronts gives an average detonation velocity of 1510 m/s. In the lower graphic, Fig. 13c a dominant frequency of ~ 5.94 kHz indicates an average detonation velocity of 1400 m/s. Both values are low compared to the Chapman-Jouguet detonation speed of 2500 m/s and indicate that this small-scale RDE is operating close to the limit of detonability.

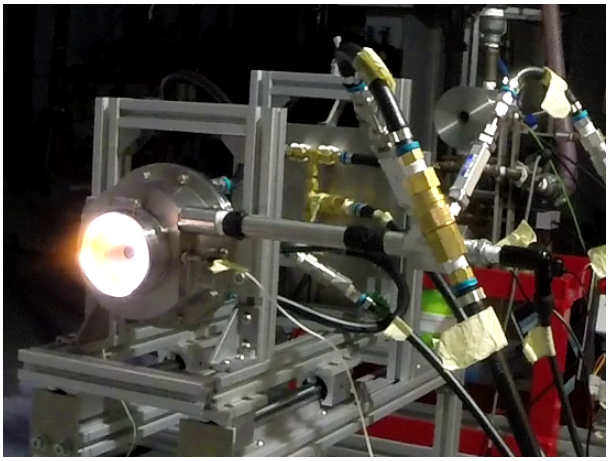

(a) $9.7\,\mathrm{g/s}$ - Bright orange flame

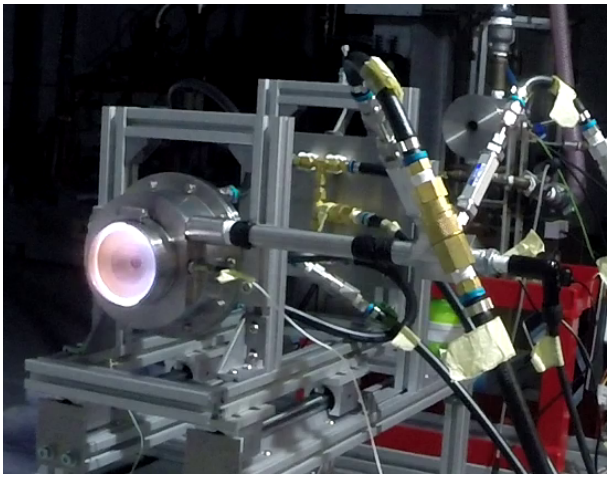

(b) $6.6\,\mathrm{g/s}$ - Weaker orange flame

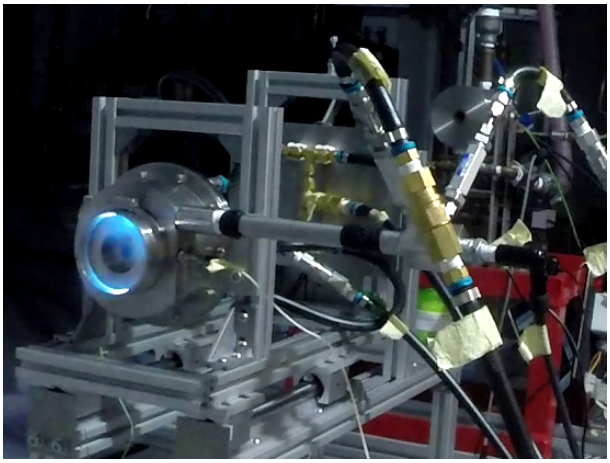

(c) $3.5\,\mathrm{g/s}$ - Blue flame

Fig 11. Flame patterns

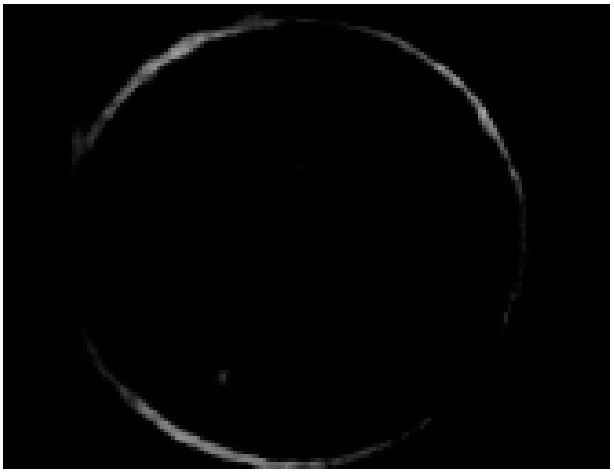

(a) $9.7\,\mathrm{g/s}$ - Three detonation heads

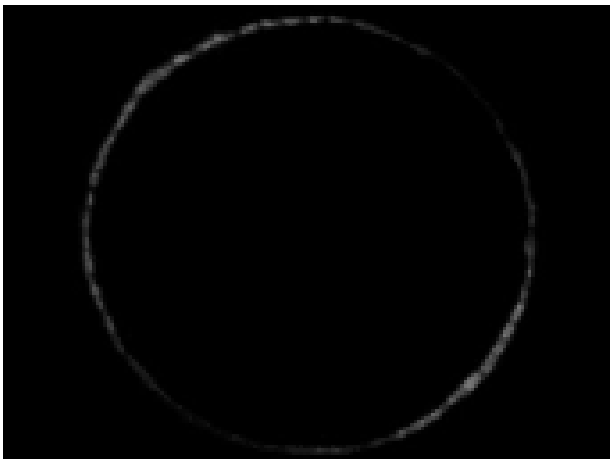

(b) $6.6\,\mathrm{g/s}$ - Two detonation heads

(c) $3.5\,\mathrm{g/s}$ - One detonation head

Fig 12. Selected frames from high speed footage, view down throat of the RDE

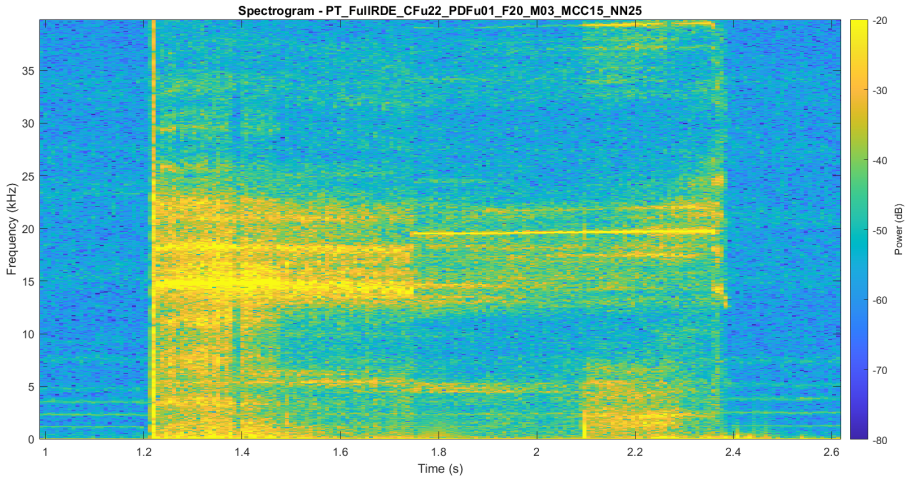

(a) $9.7\,\mathrm{g/s}$

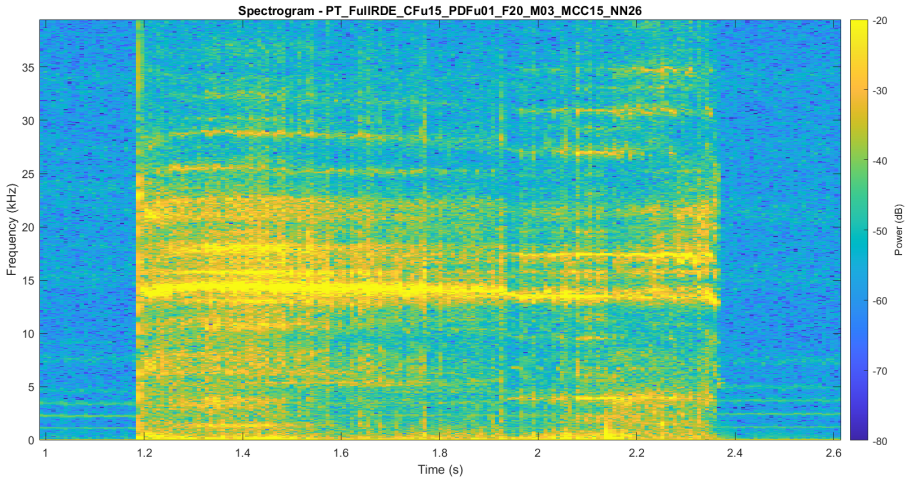

(b) $6.6\,\mathrm{g/s}$

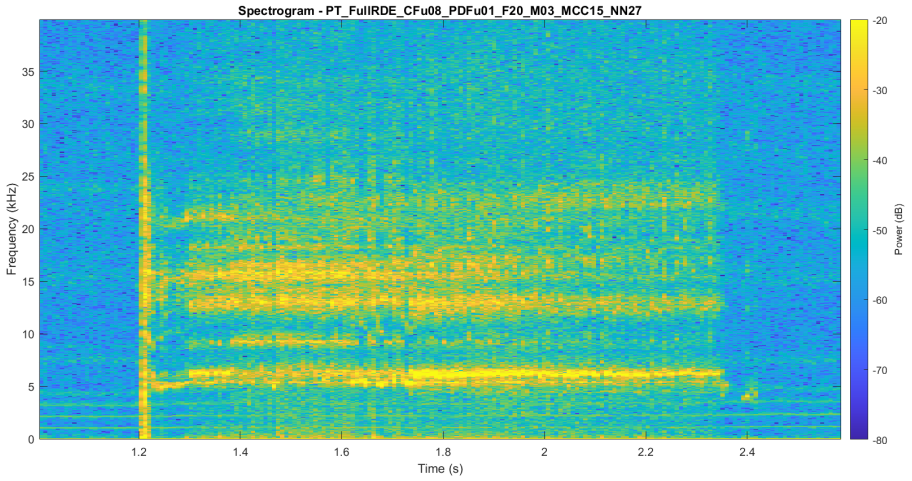

(c) $3.5\,\mathrm{g/s}$

Fig 13. Spectrograms

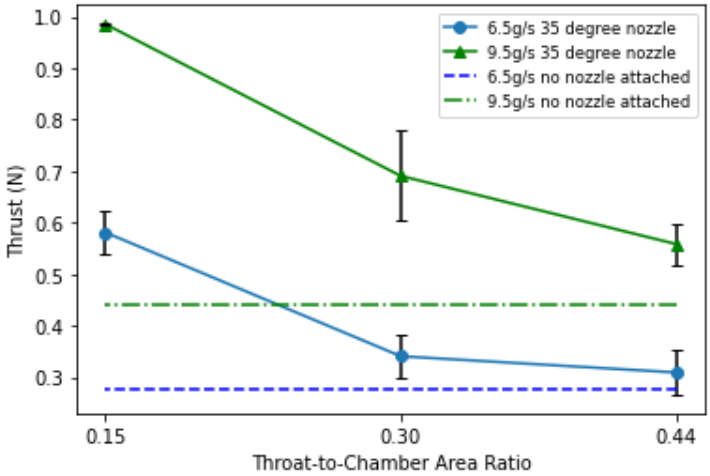

Fig 14. Recorded thrust in various configurations. Error bars show one standard deviation from the mean

3.3. Influence of constrictors and nozzle

Further testes were carried out to investigate the influence of adding the nozzle outlined in Section 2.3. Results of these tests are shown in Fig. 14. Once again, the Insert used produced a chamber of width $h = 1.2$ mm, corresponding to an axial throat area of 278.2 mm^2 and length $L = 36$ mm, and stoichiometric fuel-oxygen conditions were employed for all cases.

The dashed lines show the thrust produced without the nozzle attached, and the points indicate cases with the 35° aerospike nozzle attached, using various constrictors to reduce the throat area by a range of values. In all cases where the nozzle is attached, and some level of throat constriction takes place, the thrust is greater than that produced in the cases without the nozzle, for a the respective mass flow rate. It is apparent that with the smallest throat area of 41.1 mm^2, corresponding to a throat-to-chamber ratio of 0.15, produced the largest thrust in both cases - producing approximately $2.2\times$ greater thrust in the 9.5 g/s case and approximately $2.1\times$ for the 6.5 g/s case. It is to be expected that the attachment of a nozzle would increase thrust, through increasing exit velocity. Furthermore observations of the engine during operation with the aerospike attached showed the flames remaining attached to the nozzle, reducing off axis flow. Fotia et al. [15] found that constricting the flow drives up the local static pressure in the detonation channel, which enhances the detonation process before the nozzle converts this to pressure thrust.

The specific impulse I_{sp} of the rocket can also be evaluated as $I_{sp} = F/(\dot{m}g_o)$, where F is the thrust produced, $\dot{m}$ is the mass flow rate and g_o is the force of gravity at sea level. For the cases with the nozzle attached and smallest throat-to-chamber ratio, the specific impulse was $I_{sp} = 10.6$ s for the 9.5 g/s case and $I_{sp} = 9.11$ s for the 6.5 g/s case. These values are not particularly high, possibly highlighting the challenges of operating a miniature RDE at mass flow rates near the limit of detonability.

4. Conclusion

This paper reports what is understood to be the first successful operation of a rotating detonation engine experiments in the United Kingdom. The RDE outlined is much smaller than many of the other laboratory examples in the literature, and runs on lower mass flow rates than many that have been demonstrated before, below 10 g/s of a combined mass flow of gaseous ethylene and oxygen. The challenges in the design of an engine, such as refresh rate, of running a small engine at these mass flow rates have been outlined. The detailed chamber design, formed by two co-axial cylinders, and predetonator design and optimisation, through detonation enhancements, has been documented. The design of a modular aerospike, which allows for various nozzle configurations and throat areas, has also

been summarised.

The experimental results of varying mass flow rates, at $3.5\,\mathrm{g/s}$, $6.6\,\mathrm{g/s}$ and $9.7\,\mathrm{g/s}$ have been illustrated. An increasing number of detonation heads, observed through high speed video footage and spectral analysis of pressure transducer data, increasing from one, to two, to three for increasing mass flow rates has been reliably confirmed. Furthermore, results demonstrating the increase of thrust from the addition of a modular aerospike nozzle have been demonstrated. By varying in particular the level of constriction at the throat, the level of thrust has been found to be enhanced, as the throat-to-chamber ration was decreased from 0.44 to 0.15.

The results have confirmed that successful RDE operation for a combined mass flow as low as $3.5\,\mathrm{g/s}$ stoichiometric ethylene-oxygen is possible. Computing the detonation velocity from spectral pressure transducer data indicates that in this small-scale detonation engine detonation fronts propagate at velocities around and below 60% of the Chapman-Jouguet value. Because of the large ratio of a detonation chamber diameter of $75\,\mathrm{mm}$ versus a chamber width of only $1.2\,\mathrm{mm}$ up to three independent and temporarily even up to four (not included here) detonation heads have been observed. It is therefore believed that detonation propagation in this small-scale engine is dominated more by viscous rather than rotational effects.

Choosing a highly modular design with a lot variability among parts was found to be of critical importance to cope with manufacturing inaccuracies as well as significant uncertainties in design equations. Yet, the basic RDE design assumptions based on estimated cell size, sketched in Section 2.1, have been found to be sufficiently reliable. Not surprisingly, a first attempt in quantifying thrust from the small-scale RDE experiment has yielded comparably small overall specific impulses. The inertia of the engine and its mounting is clearly not negligible in comparison to thrust produced. Still, thrust differences could be gathered and it could be reliably established that the effect of a nozzle directly attached to the cylindrical combustion chamber outlet, in the form of constrictors, has a greater influence on produced thrust than any subsequent aerospike arrangement. Still, outlet constrictor and aerospike can be easily combined and overall thrust increases by factors > 2 have been confirmed.

An upcoming publication will focus on characterizing the operational limits of the different multi-detonation modes of propagation further depending on mass flow rate and stoichiometry more sharply.

Acknowledgements

The authors would like to thank the members of the previous three teams who worked to develop this RDE: Dougie Annesley, Mathew Bate, Jared Blackford, Lennie Chew, Nathan Clee, Adrian Garcia, David Keszthelyi, Andre Kljajic, Tan Yew Koon, James Magson, Michael Pollard, Haider Razzaq, Jack Taylor, Todor Toshkov, Cameron Ward, Daniel Wood, and Cedly Zaouia. Thanks also to Simon Klitz for his technical assistance during the test campaign.

References

[1] B. V. Voitsekhovskii, V. V. Mitrofanov, and M. E. Topchiyan, "Structure of the detonation front in gases," in *Izdatielstvo SO AN SSSR, Novosibirsk*, 1963.

[2] P. Wolański, "Detonative propulsion," *Proceedings of the Combustion Institute*, vol. 34, no. 1, p. 125–158, 2013.

[3] R. Bluemner, M. D. Bohon, C. O. Paschereit, and E. J. Gutmark, "Single and counter-rotating wave modes in an RDC," in *2018 AIAA Aerospace Sciences Meeting*, 2018.

[4] J. R. Dechert, *Development of a small scale rotating detonation engine*. Master's thesis, Air Force Institute of Technology, Wright-Patterson Air Force Base, Ohio, 2020.

[5] J. Shepherd, "Detonation database," 2002. https://shepherd.caltech.edu/detn_db/html/db.html, accessed 03-07-2021.

[6] C. B. Kiyanda, S. Connolly-Boutin, V. I. Joseph, X. Mi, H. D. Ng, and A. J. Higgins, "Small size rotating detonation engine: scaling and minimum mass flow rate," in *Proc. 26th Int. Colloquium on the Dynamics of Explosions and Reactive Systems (ICDERS)*, 2017.

[7] F. Bykovskii, S. Zhdan, and E. Vedernikov, "Continuous Spin Detonations," *Journal of Propulsion and Power*, vol. 22, pp. 1204–1216, 11 2006.

[8] J. Duvall, F. Chacony, C. Harvey, and M. Gamba, "Study of the effects of various injection geometries on the operation of a rotating detonation engine," in *AIAA SciTech Forum*, 2018.

[9] J. C. Shank, *Development and testing of a rotating detonation engine run on hydrogen and air*. Master's thesis, Air Force Institute of Technology, Wright-Patterson Air Force Base, Ohio, 2012.

[10] D. E. Paxson, "Examination of wave speed in rotating detonation engines using simplified computational fluid dynamics," in *AIAA Aerospace Sciences Meeting*, 2018.

[11] V. V. Mitrofanov and R. I. Soloukhin, "The diffraction of multifront detonation waves," *Soviet Physics Doklady*, vol. 9, p. 1055, 1965.

[12] H. James, "Fire & explosion - general," 2003. http://explosionsolutions.co.uk/110411016.pdf, accessed 16-11-2020.

[13] A. Hasson, M. Avinor, and A. Burcat, "Transition from deflagration to detonation, spark ignition, and detonation characteristics of ethylene-oxygen mixtures in a tube," *Combustion and Flame*, vol. 48, pp. 12–26, 1983.

[14] K. I. Shchelkin, "Bystroe gorenie i spinovaya detonatsiya gazov (rapid combustion and spin detonation of gases)," in *Moscow: Voyenizdat*, 1949.

[15] M. L. Fotia, F. Schauer, T. Kaemming, and J. Hoke, "Experimental study of the performance of a rotating detonation engine with nozzle," *Journal of Propulsion and Power*, vol. 32, no. 3, p. 674–681, 2016.

[16] K. Goto, J. Nishimura, and et. al, "Experimental propulsive performance and heating environment of rotating detonation engine with various throat geometries," *Journal of Propulsion and Power*, vol. 35, no. 1, pp. 213–223, 2019.